Guidelines for the Design of High-Performance Perovskite Based Solar Cells

Khaoula Amri, Rabeb Belghouthi, Michel Aillerie, Rached Gharbi

▶ **To cite this version:**

Khaoula Amri, Rabeb Belghouthi, Michel Aillerie, Rached Gharbi. Guidelines for the Design of High-Performance Perovskite Based Solar Cells. Key Engineering Materials, 2022, 922, pp.95-105. 10.4028/p-i67roy . hal-03759742

HAL Id: hal-03759742
https://hal.science/hal-03759742v1

Submitted on 24 Aug 2022

HAL is a multi-disciplinary open access archive for the deposit and dissemination of scientific research documents, whether they are published or not. The documents may come from teaching and research institutions in France or abroad, or from public or private research centers.

L'archive ouverte pluridisciplinaire **HAL**, est destinée au dépôt et à la diffusion de documents scientifiques de niveau recherche, publiés ou non, émanant des établissements d'enseignement et de recherche français ou étrangers, des laboratoires publics ou privés.

Key Engineering Materials
ISSN: 1662-9795, Vol. 922, pp 95-105
© 2022 Trans Tech Publications Ltd, Switzerland
Submitted: 2022-01-19
Revised: 2022-03-24
Accepted: 2022-03-26
Online: 2022-06-08

Guidelines for the Design of High-Performance Perovskite Based Solar Cells

Khaoula Amri[1,2,a*], Rabeb Belghouthi[3,b], Michel Aillerie[1,c] and Rached Gharbi[2,d]

[1]Université de Lorraine, CentraleSupélec, Laboratoire Matériaux Optiques, Photonique et Systèmes, LMOPS, F-57000 Metz, France

[2]Université de Tunis, Laboratoire d'Ingénierie des Systèmes Industrielles et des Energies Renouvelables, LISIER, Tunis, 1008, Tunisia

[3]Université de Valenciennes, UMR CNRS 8520, Institut d'Electronique de Microélectronique et de Nanotechnologie IEMN, dept. DOAE, F-59313 Valenciennes, France

[a,*]khaoulaomri2@yahoo.fr , [b]rabebbelghouthi@gmail.com , [c]michel.aillerie@univ-lorraine.fr ,[d]rached_gharbifr@yahoo.fr

Keywords: Perovskite; solar cells; Electron transport materials; Hole transport materials; Defect density.

Abstract. On the aim of finding the optimal solar cell structure which allows better efficiency, stability and reduced cost, a general study of a Methyl Ammonium lead Iodide $CH_3NH_3PbI_3$ based perovskite solar cell is made. Three different electron transport material compounds ETMs; TiO_2, ZnO and SnO_2 are comparatively studied considering the same hole transport material HTM, Spiro-OMeTAD. The photovoltaic parameters, i.e. the open circuit voltage (V_{oc}), the short circuit current (J_{sc}) and the power conversion efficiency (PCE) are performed considering the ETM layer thicknesses, and the defect densities in both interfaces ETM/Perovskite and Perovskite/HTM. It is found that solar cell with SnO_2 present the highest PCE for almost all configurations. Finally, the optimized cell is simulated with different organic and inorganic HTMs such as PEDOT: PSS, CuI and $CuSbS_2$.

Introduction

As efficiency of traditional silicon solar cell reaches a physical saturation level about 27-28% [1] corresponding to the maximum theoretical power conversion efficiency (PCE) with silicon, research are launched in order to find alternative materials. An emerging solar cell technology appeared with a new family of quantum dots QDs materials, perovskite solar cells are composed from mixed organic-inorganic halide ABX_3, where A is an organic cation, B is a lead or tin cation, and X is a halide anion [2]. Even if the efficiency of perovskite cells is still low compared to silicon solar cells, but its current increase, makes them one of the most promising for the near future, especially if we consider the simplicity of its manufacturing and the perspective of a low overall cost in the coming years. Their power conversion efficiency (PCE) has risen from 3.9% to certify 25.2% [3] during the last decade [4]. This large performance increase is attributed to the strong absorption coefficient of the perovskite material constituting the absorbing layer (~10^5 cm^{-1}), the long carrier diffusion length (1μm) [5] and the low exciton binding energy (~2meV).

However, there are several limiting factors that would affect the photovoltaic conversion. The main critical issue consists in the poor crystalline quality and the environmental instability [6]. Many researches are focused in order to overcome these problems and to achieve higher power conversion efficiency in PSC (Perovskite solar cells).

Best performances of perovskite solar cells are obtained with TiO_2 as electron transport material (ETM). Unfortunately, TiO_2 presents many limits, since it needs high temperature of 500°C during the annealing step to catch the crystalline rutile phase[7]. In addition, TiO_2 have low conductivity and a large amount of defects leading to inevitable huge amount of carrier fast recombination degrading the efficiency. Consequently, many researches are done to find an alternative to TiO_2. Ko

All rights reserved. No part of contents of this paper may be reproduced or transmitted in any form or by any means without the written permission of Trans Tech Publications Ltd, www.scientific.net. (#591998151-06/06/22,13:43:51)

et al. used sol-gel ZnO ETM based PSC and showed a PCE equal to about 16.5 % at 1 sun illumination [8]. In 2015, Ke *et al.* reach a higher efficiency of 17.2% with a low-temperature solution-processed nanocrystalline SnO_2 in planar PSC [9], and in 2018, Yang *et al.* achieved an efficiency of 20.79% for a PSC with SnO_2 as ETM layer [10].

Anaraki *et al.* developed a chemical bath post-treatment SnO_2 PSC which brought an efficiency of 21% [11]. On the other hand, the most popular HTM used, spiro-OMeTAD allows for a performing PSC to reach 15.98% of efficiency with open circuit voltage higher than 1.05 V as reported by Wang *et al.* [12]. Despite, this HTM presents a low hole mobility, low conductivity [13] and a high synthetic cost. Moreover, to improve the charge carrier mobility in the Spiro-OMeTAD layer, some authors considered the possibility to dope it with hygroscopic elements such as Li-TFSI or TBP, but this solution unfortunately leads to device instability under temperature [14]. To overcome those drawbacks, many HTMs with proper electronic structure can replace Spiro-OMeTAD such as PTAA [15], PEDOT: PSS [16], NiO [25], CuSCN [17]. Inorganic HTMs are characterized by a high transparency and low temperature solution processed which make them the most compatible materials for flexible PSC devices as demonstrated by Zhang *et al.* [18]. We can report results obtained with a structure built with P3HT as HTM layer and TiO_2 as ETM layer that brought a PCE of 12.4% [19]. In 2015, poly-triaylamine (PTAA) gave an interesting efficiency of 20.1% [20]. Elbohy *et al.* used PEDOT:PSS as HTM layer in an inverted $MAPbI_3$ perovskite solar cell to get an efficiency of 18.8% [21]. Other inorganic materials not expensive and with high efficiency are used, Seok *et al.* produced a spin-coated CuSCN layer as an HTM layer in mesoscopic PSCs leading to a PCE of 18.0% [22]. In order to provide a better understanding of the effect of HTM and ETM layers on the perovskite solar cell performances, we present in this contribution a comparative study pointing out the influence of electron transport materials TiO_2, ZnO and SnO_2 considering both the nature of material in terms of its physical and electronic properties and the influence of the thickness of the deposited layer. These simulations were also extended for HTMs Spiro-OMeTAD, PEDOT: PSS, Cul and $CuSbS_2$ using SnO_2 as ETM layer. Moreover, it is well-known that defect at the absorber interface in a PSC plays an important role in the global performance of solar cells. For that reason and in order to analyze their effects on the performances of the PSC, the defect densities at both interfaces ETM/Perovskite and Perovskite/HTM are finally considered in the simulation and discussion.

Basic Device Structure

The perovskite photovoltaic solar cell structure considered in this work is presented in Fig.1, It possesses a typical solar cell structure in a n-i-p planar configuration with Methyl Ammonium lead Iodide $CH_3NH_3PbI_3$ as perovskite layer sandwiched between HTM and ETM layers and external electrodes, i.e. an Au back contact layer and an ITO front contact layer.

In a first part of the modelling process, we have considered a Spiro-OMeTAD hole transport material (HTM) and analyzed the role of the electron transport material (ETM) on the performance of the cell. Three types of ETMs, TiO_2, ZnO and SnO_2 are comparatively studied. In a second part of the optimization process, we analyzed the influence of the HTM layer on the performance of the cell by keeping SnO_2 as ETM layer, and by changing the compound of the HTM layer respectively by Spiro-OMeTAD, PEDOT: PSS, Cul and $CuSbS_2$ allowing a complete analysis of the respective role of both transport layers in the performances of the perovskite solar cell.

Simulation is done under standard AM1.5 spectrum with an incident power density of 100/mW cm^2 at room temperature (300 K). Pre-factor A_α is 10^5 to obtain absorption coefficient (α) curve calculated by $\alpha = A_\alpha (hv - E_g)^{1/2}$.

The device input electronic parameters (band gap energy, dielectric, affinity, thermal velocity…) introduced in Table 1 and Table 2 and used in this simulation are obtained from reported works [23], [24], [25]. Thermal velocity of electron and hole is 10^7 cm/s. Bulk defect density, 2.5×10^{13} cm^{-3} is used in both perovskites with Gaussian distribution having characteristic energy of

0.1 eV and situated in the middle of the bandgap. The type of defect is neutral defect with the capture cross section of electrons and holes are $2.0 \times 10^{-14}\,cm^{-2}$.

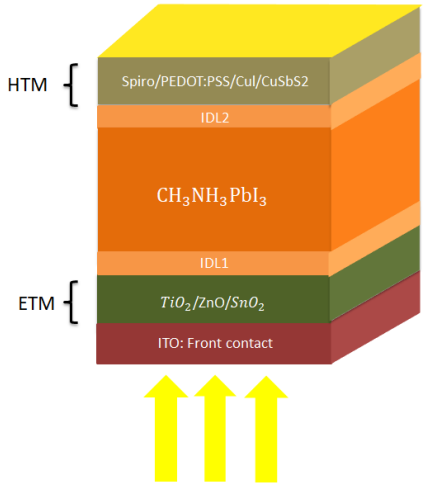

Figure 1. Schematic structure of simulated perovskite solar cell.

Table 1. Simulation parameters of the ETMs and the perovskite layers.

Parameters	TIO2	SnO2	ZnO	IDL2	MAPbI3	IDL1
Thickness(nm)	100	100	100	10	400	10
E_g (eV)	3.2	3.6	3.3	1.55	1.55	1.55
χ (ev)	4	4	4	3.9	3.9	3.9
ε_r	100	8	9	10	10	10
N_c ($1/cm^3$)	$2.2*10^{18}$	$3.16*10^{18}$	$2.2*10^{18}$	$2.76*10^{18}$	$2.76*10^{18}$	$2.76*10^{18}$
N_v ($1/cm^3$)	$1.8*10^{19}$	$2.5*10^{19}$	$1.8*10^{19}$	$3.9*10^{18}$	$3.9*10^{18}$	$3.9*10^{18}$
μ_n (cm^2 /Vs)	0.006	15	300	15	15	15
μ_p (cm^2 /Vs)	0.006	0.1	1	15	15	15
N_A ($1/cm^3$)				10^{11}	10^{11}	10^{11}
N_D ($1/cm^3$)	10^{19}	10^{19}	10^{19}			
N_t ($1/cm^3$)	10^{15}	10^{15}	10^{15}	10^{17}	$2.5*10^{13}$	10^{17}

Table 2. Simulation parameters of the HTMs layer.

Parameters	Spiro-OMeTAD	PEDOT PSS	CuI	$CuSbS_2$
Thickness(nm)	200	200	200	200
E_g (eV)	3	2.2	2.98	1.58
χ (ev)	2.45	2.9	2.1	4.2
ε_r	3	3	6.5	14.6
N_c ($1/cm^3$)	$2.2*10^{18}$	$2.2*10^{18}$	$2.5*10^{19}$	$2*10^{18}$
N_v ($1/cm^3$)	$1.8*10^{19}$	$1.8*10^{19}$	$2.5*10^{19}$	10^{19}
μ_n (cm^2 /Vs)	0.0002	0.01	$1.69*10^{-4}$	49
μ_p (cm^2 /Vs)	0.0002	0.003	$1.69*10^{-4}$	49
N_A ($1/cm^3$)	$2*10^{18}$	10^{21}	10^{18}	10^{18}
N_D ($1/cm^3$)				
N_t ($1/cm^3$)	10^{15}	10^{15}	10^{15}	10^{15}

Influence of ETM composition and thickness on PSC functional parameters

As previously mentioned, we first consider a PSC composed by a 400nm thick absorber layer of $CH_3NH_3PbI_3$, a 200nm thick HTM layer of Spiro-OMeTAD and analyze the role of the ETM layer on the performance of the cell through the consideration of three types of ETM, TiO_2, ZnO and SnO_2, respectively. We report the results of simulations for these three ETM types as function of the

thickness of the ETM layer in Fig. 2**.** The presented results are the open circuit voltage (V_{oc}), short circuit current density (J_{sc}) and PCE. The range of the thickness of the ETM layer, varying between 90nm and 450nm matches to the standard thickness generally considered in researches and pre-industrial PSC.

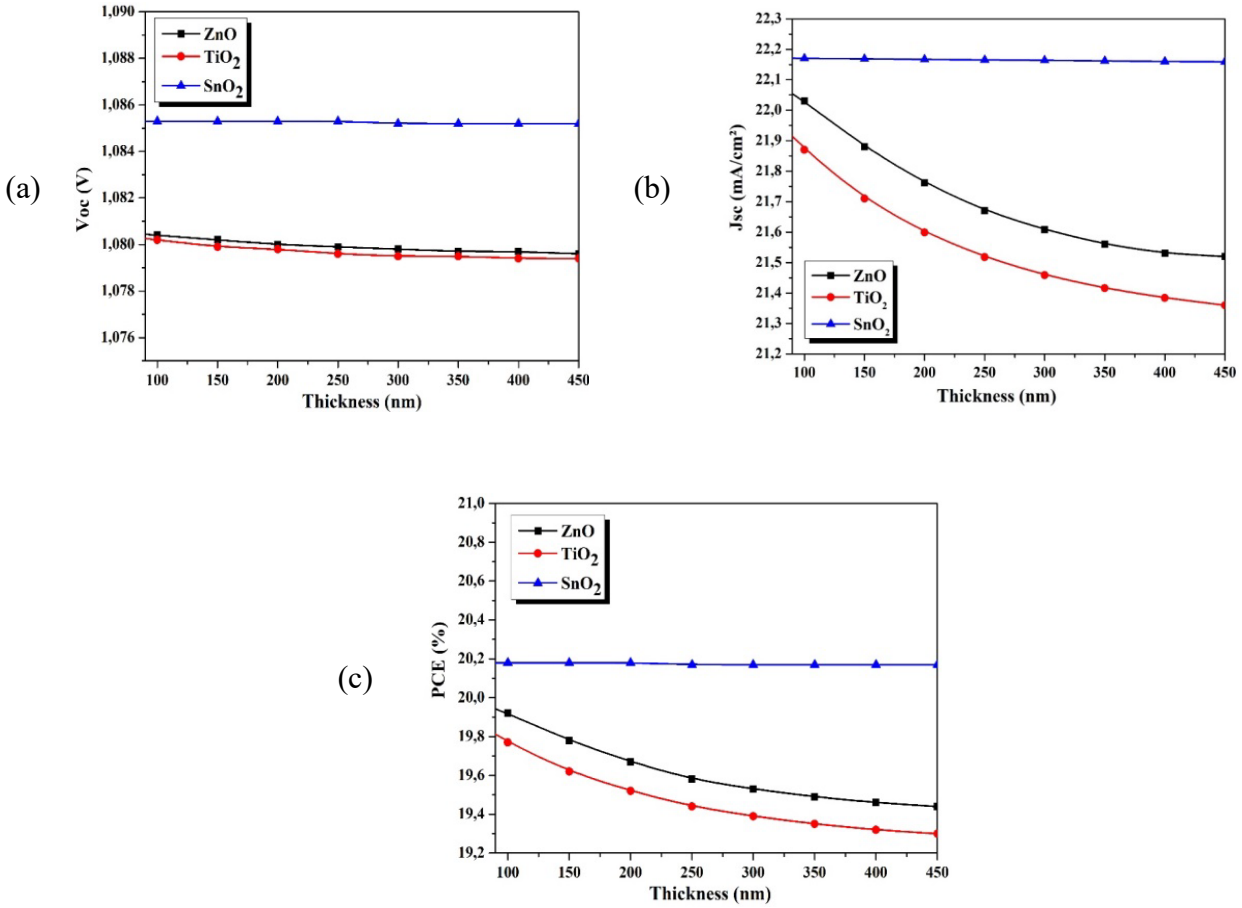

Figure 2. Photovoltaic parameters as function of ETM thickness (a) Open circuit voltage V_{oc} (b) photo-current density J_{sc} (c) The solar cell efficiency.

We observe that whatever is the thickness of the ETM layer, V_{oc}, J_{sc} and PCE are favor with SnO_2 ETM layer, the worst being for the TiO_2 one. Moreover, the behavior of these functional parameters with the thickness of the ETM layer is not the same for the three compounds: it decreases with the increase of the thickness in case of TiO_2 and ZnO, but is quasi-constant in SnO_2. All numerical results proved that TiO_2 is more sensitive compared to ZnO and SnO_2. The particular behavior of TiO_2 compared to the two other ones is attributed to its lower transmittance and lower electron mobility. Thus, the increase of the ETM thickness degrades the performance of the solar cells with TiO_2 and ZnO ETM layers. The absorption of incident solar energy by TiO_2 or ZnO ETM layers drops the rate of charge generation and collection inducing a decrease of J_{sc}. However, in case of SnO_2 ETM layer, and due to its higher transparency, the active layer keeps a quasi-constant absorption level in the considered thickness range of the ETM layer, thus having no significant influence in the behavior of J_{sc}. Moreover, owing to the high mobility and carrier concentration of SnO_2, by increasing the thickness of ETM, the series resistance decreases. Our results match with different experimental works and numerical simulations [26] [27] [28] showing the same behavior of the three ETMs used.

Impact of defect density on solar cell performances

The structural mismatch of two different materials leads to initiate the interfacial defects, which cause the charge recombination in the PSCs. In the current contribution, we consider defects at both ETM/absorber and absorber/HTM interfaces allowing our simulation to approach the real behavior of cells. For that, we introduce two layers, named IDL1 and IDL2 with a fixed thickness equal to 10nm, and analyze the influence of the defect density in the range 10^{13} cm^{-1} to 10^{21} cm^{-1}, which corresponds to the range of defect density commonly experimentally admitted in this type of cells [29]. In the modeling PSC structure, TiO_2, ZnO and SnO_2 are respectively considered as ETM layers, with a Spiro-OMeTAD as HTM layer having a thickness equal to 200nm. The behavior of the functional parameters obtained by simulations of such structures as function of defect concentrations in IDL1 and IDL2 is reported in Fig. 3.

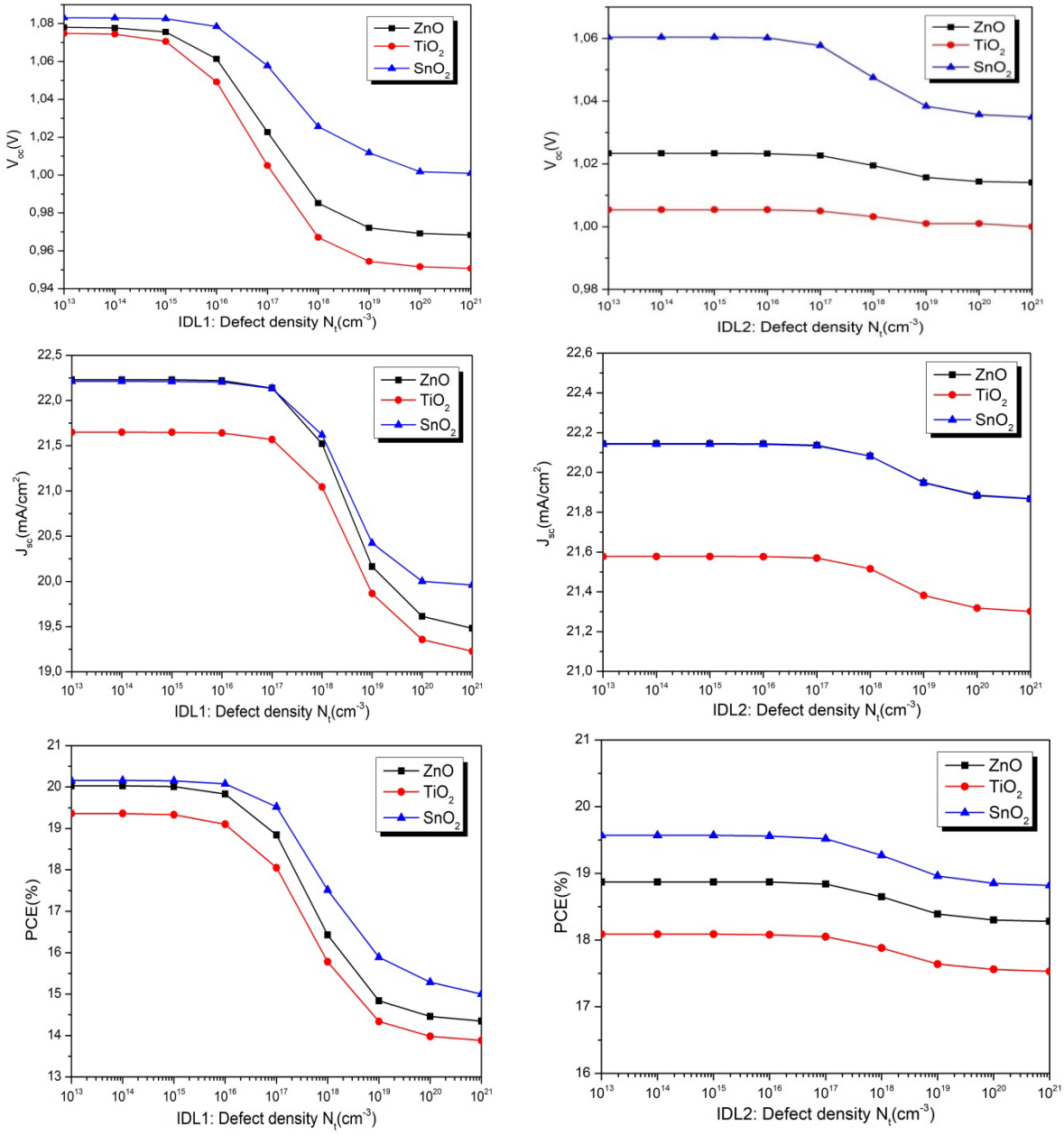

Figure 3. Effect of defect density in a) ETM/absorber IDL1 with [IDL2]=$10^{17}cm^{-3}$ and b) absorber/HTM IDL2 with [IDL1]=$10^{17}cm^{-3}$ on PSC parameters.

As it can be understood from Fig. 3, the interface quality at ETM/absorber has the biggest impact on the solar cell parameters than the absorber/HTM interface. This behavior confirmed results of simulations published by Minemoto *et al.* using the same type of cell structure [30]. In fact, the cell

being illuminated on the front side where the ETM layer is located, the generation of electron - holes pairs is maxima in this region. Gradually through the layers, mainly due to the high absorption of the absorber, the possibilities of generation of carriers decrease by going toward the back side. Thus, in an optimization process of the efficiency of a solar cell, wider possibilities are offer when special care are brought to the ETM/absorber interface, hugely dependent of the defect density, compared with the improvement possibilities offer by a change in the parameters of the absorber/HTM interface.

Finally, the results presented in Figs. 3 confirm that PSC integrating SnO_2 ETM layer have the highest performances compared to PSC with TiO_2 or ZnO ETM layer, even if the relative changes of these parameters are in the same amplitude range with defect densities. This behavior is closely link to the better energy band alignment between SnO_2 and perovskite, providing low interface states resistances in the global structure of the PSC.

Influence of HTM composition and thickness on PSC functional parameters

In both previous sections, we notice that the performance is higher in PSC with SnO_2 ETM layer than in PSC with ZnO or TiO_2 ETM layer, and this, regardless the thickness of this layer or of the absorber layer. Moreover, we also know that HTM layers should have some specifications in order to obtain the optimum efficiency. We can cite high hole mobility that allows to reduce series resistances, energy levels that should match with HOMO and LOMO of perovskite used and HTM work function that should be matching with valence band of perovskite which helps obtaining high V_{oc} [31].

Thus, in this section, we continue the process of optimizing the performance of the PSC by discussing, now, the influence of the HTM composition and thickness on the functional parameters of the cell. Thus, taking into account the previous results, we retain a $CH_3NH_3PbI_3$ PSC with SnO_2 ETM layer. The various compounds for HTM layers that we consider are Spiro-OMeTAD, PEDOT:PSS, Cul and CuSbS2, currently suggested in literature. The results of the simulation process with these four compounds as function of the thickness of the HTM layer in the range 50-250 nm are presented in Fig. 4.

We clearly see in Fig. 4 that the responses of the considered functional parameters depend on the thickness and the type of HTM used in the device.

HTMs used in this simulation belong in two material families, i.e. organic (Spiro-OMeTAD and PEDOT:PSS), and inorganic (Cul and CuSbS2). Each one exhibits different behaviors in the photo-conversion process and thus in the response and performance of the resulting solar cell. In case of organic solar cells, V_{oc} increases by raising the HTM thickness while J_{sc} and PCE decrease. These behaviors are attributed to the relatively low conductivity and charge carriers mobility of those materials responsible of the increase of the resistance of the layer. In contrast, inorganic materials have high hole mobility and conductivity, and in this case, HTM layer allows a high V_{oc} for the PSC. In term of layer thickness, we can note that for the case of Spiro-OMeTAD, PEDOT:PSS and Cul, the power conversion efficiency is improved in thinner HTM due to lower series resistances and reduced time for holes to move toward Au electrode. We note that this observed behavior was also obtained by Raoui *et al.* in PSC structures with different HTM candidates [24].

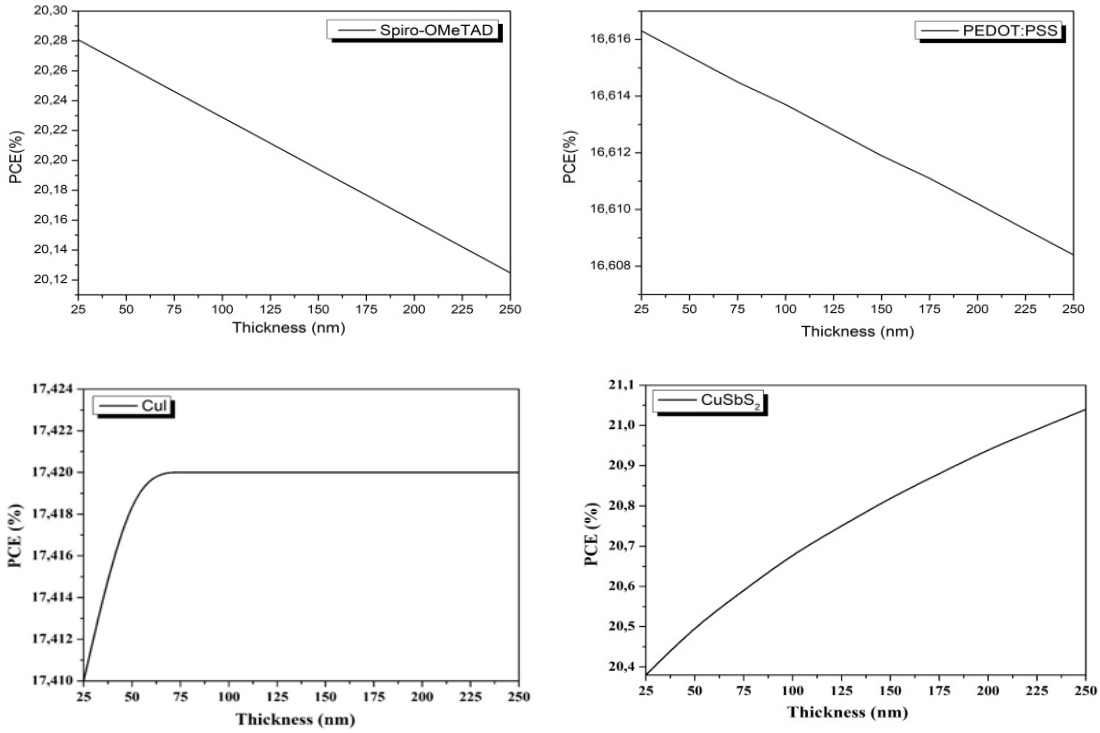

Figure 4. Influence of the HTM layer compound and thickness on PSC functional parameters with SnO_2 ETM layer.

Final Applicable Guidelines

Following the study made above by analyzing the different effects of the ETM, HTM absorber thicknesses as well as the defect densities at the interfaces IDL1 and IDL2 on the solar cell parameters, we can obtain the optimized values of the three layers that allow the best efficiency of the PSC. The device was simulated using the three ETMs (100 nm), the Spiro-OMeTAD (200 nm) as HTM layer, $CH_3NH_3PbI_3$ (400 nm) as absorber layer and by fixing the defect density of IDL1 and IDL2 at 10^{17} cm^{-3}. The I-V curve of the three ETMs is shown in Fig. 5 and the solar cell performances obtained are mentioned in Table 4, SnO_2 shows the best power conversion efficiency.

Even if TiO_2 has been intensively used as ETM layer for $CH_3NH_3PbI_3$ perovskite based solar cells in commercial devices, thanks to its good efficiency in a planar n-i-p structure, the current study proves that new alternatives exist to replace TiO_2 by ZnO or SnO_2 with an improved efficiency.

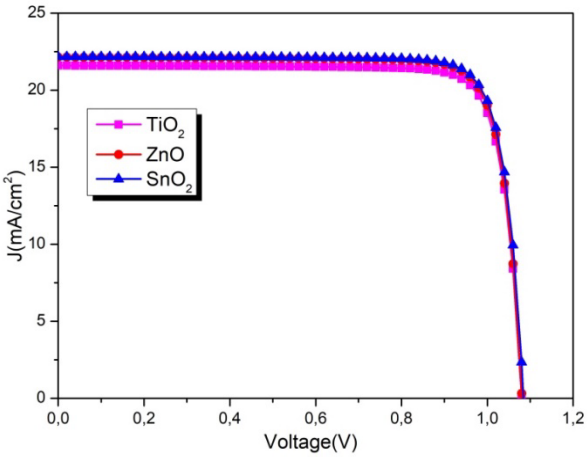

Figure 5. Simulated J-V curves of perovskite solar cells with 100 nm thick ZnO, TiO2, and SnO2 ETL layer.

Table 4. Comparative photovoltaic properties of TiO_2, ZnO and SnO_2 ETMs for $MAPbI_3$ perovskite based solar cell with optimized thickness.

ETM	V_{oc} (V)	J_{sc} (mA/cm^2)	FF (%)	PCE (%)
TiO_2	1.08	21.59	83.7	19.53
ZnO	1.08	22.13	83.68	20.01
SnO_2	1.85	22.17	83.85	20.16

However, TiO_2 based PSC are more expensive and requires a highest annealing temperature which doesn't allow its deposition on flexible support [32]. Thus, we can cite, at first, the development of ETM layer in ZnO with higher electron mobility than TiO_2 [33] [34] and better photon transmission to the perovskite absorber layer [35] and also with capability to be applied to flexible perovskite solar cells. At second, we can cite layer based on SnO_2 being the subject of recent studies owing to its high electron mobility, its matching energy level with mixed perovskite including $MAPbI_3$. Moreover, SnO_2 layer can be deposited at low temperature (<200°C) with excellent electrical properties [36] and stable cell performance [37]. In addition, the presence of this layer reveals a supplementary advantage as shown by Jiang *et al.* [38] and Song *et al.* [39] being the low acidity resistance of SnO_2 assumed the best ETM durability of the perovskite solar cell device.

Conclusion

The functional parameters resulting in the efficiency of $CH_3NH_3PbI_3$ perovskite solar cells, was analyzed as function of the nature of compounds used, as well as the thickness of the ETM and HTM layers of the considered structure. Since in real devices, the important defect is located at the perovskite front and back interfaces, we have introduced two layers ETM/absorber (IDL1) and absorber/HTM (IDL2). Defect density in IDL1 interface influence more than IDL2 interface on the solar cell parameters. All discussions are based on a comparison with results obtained in literature.

For the ETM layer, we have considered three different electron transport materials (ZnO, TiO_2 and SnO_2), corresponding to real solutions experimentally and commercially tested. Among these possibilities for the ETM layer of the cell, results show that SnO_2 based ETM layer, 100nm thick, allows obtaining the best PSC performances. The efficiency, achieving 20.16% is attributed to the higher transparency and higher carrier mobility in the ETM layer and a complete photon absorption in the perovskite layer.

The effect of different organic and inorganic HTM layers has also been studied. Outcomes proves that inorganic HTM layers are most effective with a high mobility of holes and a best matching energy level with the valence band of perovskite. SnO_2 based device shows the most promising results proved by the invariance of solar cell efficiency due to interface states.

References

[1] NREL, Annual Technology Baseline Electricity Data 2020. https://www.nrel.gov/news/program/2020.

[2] R. Chang, J. Zhang, S. Ullah, Z. Zhu, Y. Chen, H. Guo, J. Gu, The Cesium doping using the nonstoichiometric precursor for improved CH3NH3PbI3 perovskite films and solar cells in ambient air, Thin Solid Films 690 (2019) 137-563.

[3] NREL, Annual Technology Baseline Electricity Data 2019. https://www.nrel.gov/news/program/2019.

[4] M. A. Green, A. H. Baillie, H. J. Snaith, The emergence of perovskite solar cells, Nature Photonics 8 (2014) 506 - 14.

[5] Q. Lin, A. Armin, R. C. R. Nagiri, P. L. Burn, P. Meredith, Electro-optics of perovskite solar cells, Nat. Photon. 9(2015) 106-112.

[6] G. Niu, W. Li, J. Li, X. Liang, L. Wang, Enhancement of thermal stability for perovskite solar cells through cesium doping, RSC Advances 7 (2017), 17473-17479.

[7] H. L. Y. Guan, J. Y. S. L. Xue, L. H. Sheng, Q. F. Cheng, X. L. Chang, J. Lia, High-thermoelectric performance of TiO2-x fabricated under high pressure at high Temperatures, Journal of Materiomics 4(2017) 286-292

[8] Y. Ko, Y. Kim, S. Y. Kong, S. C. Kunnan, Y. Jun, Improved performance of sol–gel ZnO-based perovskite solar cells via TiCl4 interfacial modification, Solar Energy Materials and Solar Cells 183 (2018) 157–163.

[9] W. J. Ke, G. J. Fang, Q. Liu, L. B. Xiong, P. L. Qin, H. Tao, J. Wang, H. W. Lei, B. R. Li, J. W. Wan, G. Yang, Y. F. Yan, Low-Temperature Solution-Processed Tin Oxide as an Alternative Electron Transporting Layer for Efficient Perovskite Solar Cells, J. Am. Chem. Soc. 137(2015) 6730–6733.

[10] G. Yang, C. Chen, F. Yao, Z. Chen, Q. Zhang, X. Zheng, G. Fang, Effective Carrier-Concentration Tuning of SnO2 Quantum Dot Electron-Selective Layers for High-Performance Planar Perovskite Solar Cells, Advanced Materials 30(2018) 1706023.

[11] E. H. Anaraki, A. Kermanpur, L. Steier, K. Domanski, T. Matsui, W. Tress, M. Saliba, A. Abate, M. Grätzel, A. Hagfeldt, J. Correa-Baena, Highly efficient and stable planar perovskite solar cells by solution-processed tin oxide, Energy Environ. Sci. 9(2016) 3128-3134.

[12] F. Wang, S. Bai, W. Tress, A. Hagfeldt, F. Gao, Defects engineering for high-performance perovskite solar cells, npj Flex Electron 22 (2018) 2-22.

[13] W. H. Nguyen, C. D. Bailie, E. L. Unger, M. D. McGehee, Enhancing the Hole-Conductivity of Spiro-OMeTAD without Oxygen or Lithium Salts by Using Spiro(TFSI)2 in Perovskite and Dye-Sensitized Solar Cells, Journal of the American Chemical Society 136(2014), 10996–11001.

[14] F. Lamberti, T. Gatti, E. Cescon, R. Sorrentino, A. Rizzo, E. Menna, L. Franco, Evidence of Spiro-OMeTAD De-doping by tert-Butylpyridine Additive in HoleTransporting Layers for Perovskite Solar Cells, Chem. 5(2019) 1806-1817.

[15] S. Ryu, J. H. Noh, N. J. Jeon, Y. C. Kim, W. S. Yang, J. W. Seo, S. I. Seok, Voltage output of efficient perovskite solar cells with high open-circuit voltage and fill factor, Energy Environ. Sci. 7(2014) 2614-2618.

[16] K. H. Hendriks, J. J. Van Franeker, B. J. Bruijnaers, J. A. Anta, M. M. Wienk, R. A. J. Janssen, 2-Methoxyethanol as a new solvent for processing methylammonium lead halide perovskite solar cells, J. Mater. Chem 5(2017) 2346–2354.

[17] V. E. Madhaven, I. Zimmermann, C. R. Carmona, G. Grancini, M. Buffiere, A. Belaidi, M. K. Nazeeruddin, Copper Thiocyanate Inorganic Hole-Transporting Material for High-Efficiency Perovskite Solar Cells, ACS Energy Lett. 1(2016) 1112–1117.

[18] H. Zhang, J. Cheng, F. Lin, H. He, J. Mao, K. S. Wong, W. C. H. Choy, Pinhole-Free and Surface-Nanostructured NiOx Film by Room-Temperature Solution Process for High-Performance Flexible Perovskite Solar Cells with Good Stability and Reproducibility, ACS Nano 10(2016) 1503–1511.

[19] A. Abrusci, S. D. Stranks, P. Docampo, H. L. Yip, A. K. Y. Jen, H. J. Snaith, High-Performance Perovskite-Polymer Hybrid Solar Cells via Electronic Coupling with Fullerene Monolayers, Nano Lett. 13(2013) 3124–3128.

[20] W. S. Yang, J. H. Noh, N. J. Jeon, Y. C. Kim, S. Ryu, J. Seo, S. I. Seok, High-performance photovoltaic perovskite layers fabricated through intramolecular exchange, Science 348(2015) 1234 -1237.

[21] H. Elbohy, B. Bahrami, S. Mabrouk, K. M. Reza, A. Gurung, R. Pathak, M. Liang, Q. Qiao, K. Zhu, Tuning Hole Transport Layer Using Urea for High-Performance Perovskite Solar Cells, Adv. Funct. Mater 29(2018), 1806740.

[22] M. Jung, Y. C. Kim, N. J. Jeon, W. S. Yang, J. Seo, J. H. Noh, S. I. Seok, Thermal Stability of CuSCN Hole Conductor-Based Perovskite Solar Cells, Chem. Sus. Chem. 9(2016) 2592-2596.

[23] B. K. Menariya, R. Ameta, S. C. Ameta, A Comparative Study on Photocatalytic Activity of ZnO, SnO2 and ZnO-SnO2 Composites, J. Chem. Sci. 15(2017) 2581-5423.

[24] Y. Raoui, H. Ez-Zahraouy, N. Tahiri, O. El Bounagui, S. Ahmad, S. Kazim, Performance analysis of MAPbI3 based perovskite solar cells employing diverse charge selective contacts: Simulation study, Solar Energy 193(2019) 948–955.

[25] A. Ali, L. M. Chepyga, L. S. Khanzada, A. Osvet, C. J. Brabec, M. Batentschuk, Effect of water vapor content during the solid state synthesis of manganese-doped magnesium fluoro-germanate phosphor on its chemistry and photoluminescent properties, Opt. Mat. 99(2020) 0925-3467.

[26] K. R. Adhikari, S. Gurung, B. K. Bhattarai, B. M. Soucase, Comparative study on MAPbI3 based solar cells using different electron transporting materials, Physica Status Solidi 13(2015), 13–17.

[27] F. Azri, A. Meftah, N. Sengouga, Electron and hole transport layers optimization by numerical simulation of a perovskite solar cell, Solar Energy 181(2019) 372–378.

[28] E. Karimi, S. M. B. Ghorashi, The Effect of SnO2 and ZnO on the Performance of Perovskite Solar Cells, Journal of Electronic Materials. 49(2020), 364–376.

[29] R.Rajeswari, M.Mrinalini, S.Prasanthkumar, L.Giribabu, Emerging of Inorganic Hole Transporting Materials For Perovskite Solar Cells, Chem. Rec. 17(2017) 1–20.

[30] T. Minemoto, M. Murata, Device modeling of perovskite solar cells based on structural similarity with thin film inorganic semiconductor solar cells, J. Applied Physics 116(2014) 054505.

[31] A .S. Chouhan, N. P. Jasti, S. Avasthi, Effect of interface defect density on performance of perovskite solar cell: Correlation of simulation and experiment, Materials Letters, 221 (2018) 150–153.

[32] H. Liu, Z. Huang, S. Wei, L. Zheng, L. Xiao, Q. Gong, Nano-structured electron transporting materials for perovskite solar cells, Nanoscale 8(2016) 6209–6221.

[33] X. Yin, P. Chen, M. Que, Y. Xing, W. Que, C. Niu, J. Shao, Highly Efficient Flexible Perovskite Solar Cells Using Solution-Derived NiOx Hole Contacts, ACS Nano 10(2016) 3630–3636.

[34] A. Bedia, F. Z. Bedia, M. Aillerie, N. Maloufi, S. O. S. Hamady, O. Perroud, B. Benyoucef, Optical, electrical and structural properties of nano-pyramidal ZnO films grown on glass substrate by spray pyrolysis technique, Optical Materials 36(2014) 1123-1130.

[35] Y. Chen, Y. Sun, J. Peng, J.Tang, K. Zheng, Z. Liang, 2D Ruddlesden–Popper Perovskites for Optoelectronics, Adv. Mater. 30(2018) 1703487.

[36] Z. L. Tseng, C. H. Chiang, C. G. Wu, Surface Engineering of ZnO Thin Film for High Efficiency Planar Perovskite Solar Cells, Scientific reports 5(2015) 13211.

[37] S. Song, G. Kang, L. Pyeon, C. Lim, G. Y. Lee, T. Park, J. Choi, Systematically Optimized Bilayered Electron Transport Layer for Highly Efficient Planar Perovskite Solar Cells (η = 21.1%), ACS. Energy Lett. 2(2017) 2667.

[38] Q. Jiang, Z. Chu, P. Wang, X. Yang, H. Liu, Y. Wang, Z. Yin, J. Wu, X. Zhang, J. You, Planar-Structure Perovskite Solar Cells with Efficiency beyond 21%, Adv. Mater 29(2017) 1703852.

[39] J. Song, E. Zheng, J. Biang, X. F. Wang, W. Tian, Y. Sanehira, T. Miyasaka, Low-temperature SnO2-based electron selective contact for efficient and stable perovskite solar cells, J. Mater. Chem 3(2015) 10837.